THE JOURNAL OF PHYSICAL CHEMISTRY Letters

pubs.acs.org/JPCL

Phase Separation on a Phospholipid Membrane Inducing a Characteristic Localization of DNA Accompanied by Its Structural Transition

Ayako Kato,[†] Akihiko Tsuji,[‡] Miho Yanagisawa,[§] Daisuke Saeki,[§] Kazuhiko Juni,[†] Yasunori Morimoto,[†] and Kenichi Yoshikawa*[,‡,§]

[†]Graduate School of Pharmaceutical Sciences, Josai University, Sakado 350-0295, Japan, [‡]Spatio-Temporal Order, ICORP, Japan Science and Technology Agency, Kyoto 606-8502, Japan, and [§]Department of Physics, Graduate School of Science, Kyoto University, Kyoto 606-8502, Japan

ABSTRACT We report the coupling of phase separation on a phospholipid membrane with a structural transition of giant DNA. We performed single-DNA measurements in the presence of cell-sized giant unilamellar vesicles (GUV) composed of dioleoylphosphatidylcholine (DOPC), phosphatidylethanolamine (PE), and cholesterol. We observed the effect of phase separation of the membrane by changing PE from dioleoylphosphatidylethanolamine (DOPE) to dipalmitoylethanolamine (DPPE), which corresponds to a change from a homogeneous single phase to two segregated phases of liquid-ordered and liquid-disordered states on the membrane. In the homogeneous membrane, DNA molecules exhibited a compact conformation in aqueous solution containing a physiological concentration of Mg^{2+} and polyamine, without attaching to the membrane surface. In contrast, in the membrane that was segregated into two domains, DNA molecules were adsorbed onto the liquid-ordered phase that was rich in DPPE by taking an elongated conformation.

SECTION Biophysical Chemistry

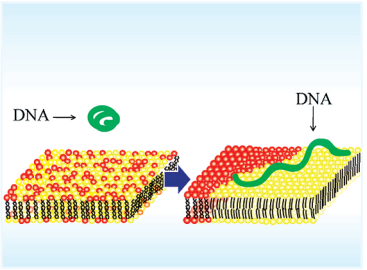

The cell plasma membrane is composed of various kinds of phospholipids, together with glycolipids and cholesterol. It has been revealed that the distribution and lateral organization of these lipids in the membrane plane is not uniform, and various microdomains such as lipid rafts that show lipid compositions different from those of other parts of the membrane are formed temporarily and dynamically.[1−4] This dynamical and heterogeneous structure is a critical aspect of the cell and intracellular membranes and provides a surface field on which various cellular molecular reactions and events take place.[5−7] It has been shown that giant (≥1 μm) unilamellar vesicles (GUV) formed from a ternary mixture of a phospholipid with saturated acyl chains, a phospholipid with unsaturated acyl chains, and cholesterol undergo phase separation into two micrometer-scale domains, a liquid-disordered phase (L_d) enriched in the unsaturated phospholipid and a liquid-ordered phase (L_o) rich in the saturated phospholipid and cholesterol.[8−11] The coexistence of different phases on the GUVs serves as a good model for studying the roles of heterogeneous structures on the membrane in the function of cellular membranes and their mimics. In this study, we examined the effects of phase separation in GUVs composed of phosphatidylcholine (PC), phosphatidylethanolamine (PE), and cholesterol, which mimics the composition of cellular membranes, on the interaction of long DNA molecules with the membrane.

We prepared GUVs composed of dioleoylphosphatidylcholine (DOPC), dioleoylphosphatidylethanolamine (DOPE) or dipalmitoylphosphatidylethanolamine (DPPE), and cholesterol (Chol) by the natural swelling method.[12] A head-group-labeled fluorescent phospholipid (rhodamine-DOPE), which preferentially resides in the L_d phase,[10,13] was also incorporated into the membrane to reveal the domain structures in GUVs. Figure 1 shows confocal laser scanning fluorescence microscope images of GUVs at room temperature (the focus was on the upper surface of each GUV). When GUVs were formed from a ternary mixture of 1:1 DOPC/DOPE and 37 mol % cholesterol, the distribution of rhodamine-DOPE showed that there was one homogeneous phase throughout the membrane (Figure 1Aa). In contrast, on GUVs formed with 1:1 DOPC/DPPE and 37 mol % cholesterol (Figure 1Ca), two micrometer-scale phases (regions with high and low fluorescence intensities) coexisted on the membrane. Similar fluorescence images showing coexistence of the two phases have been reported for GUVs composed of DOPC, DPPC, cholesterol, and rhodamine-DOPE.[10,14,15] On these GUVs, the greater fluorescence intensity region has been assigned to be the L_d domain that is rich in unsaturated DOPC, and the lower fluorescence region is the L_o domain that is rich in saturated DPPC and cholesterol. For the present GUVs composed of DOPC, DPPE, and cholesterol,

Received Date: October 5, 2010
Accepted Date: November 10, 2010
Published on Web Date: November 15, 2010

DOI: 10.1021/jz101376m | *J. Phys. Chem. Lett.* **2010**, *1*, 3391–3395

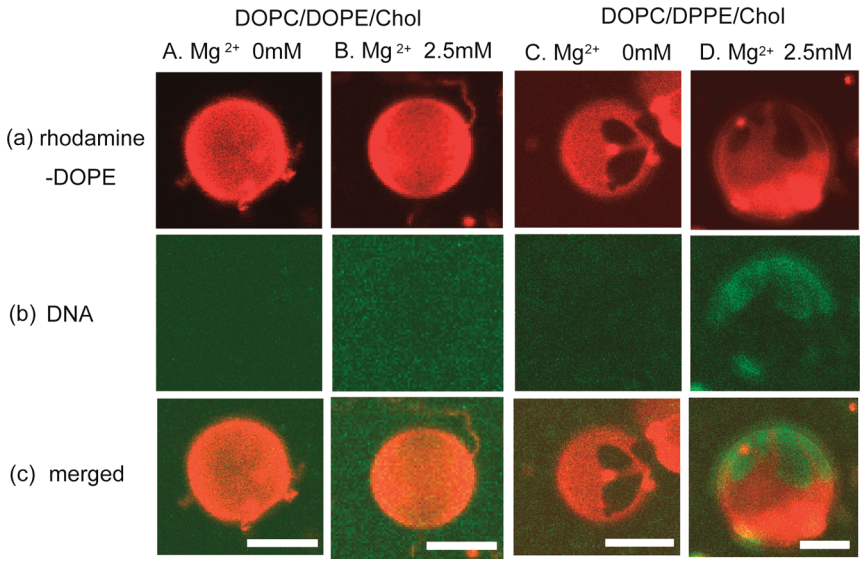

Figure 1. Confocal laser scanning fluorescence microscope images of GUVs. GUVs composed of DOPC/DOPE/Ch/rhodamine-DOPE (3:3:3.5:0.06, molar ratio) or DOPC/DPPE/Ch/rhodamine-DOPE (3:3:3.5:0.06) were prepared, and fluorescent (YOYO-1)-labeled T4 DNA was then added to the GUV solution in the absence or the presence (2.5 mM) of Mg^{2+}. The two (488 nm for excitation of YOYO-1 and 543 nm for excitation of rhodamine) laser lines were simultaneously used to irradiate the samples, and the rhodamine-DOPE (a) and T4 DNA (b) images were obtained simultaneously at each fluorescence channel. The focus was on the upper surface of each GUV with a slice width of 5.5 μm. In images Ab, Bb, and Cb, there was little signal on the GUV, which indicates that T4 DNA was not bound to the GUV (T4 DNA was present in the aqueous solution). The image acquisition time was 1.57 s. (c) Merged image of (a) and (b). Scale bar, 10 μm.

it can be considered that the membranes were segregated into the L_d phase rich in DOPC (greater fluorescence intensity region) and the L_o phase rich in DPPE and cholesterol (lower fluorescence region) (the chain melting temperature of DPPE (61 °C) is far above room temperature).

It has been reported that DNA is bound to a membrane composed of zwitterionic phospholipids such as PC and PE in the presence of a divalent metal cation such as Mg^{2+} or Ca^{2+}.[16−20] We added bacteriophage T4 DNA (166 kilo base-pairs) labeled with the fluorescent dye YOYO-1 to the GUVs (Figure 1B and D; see also images of other GUVs in Figure S1 in the Supporting Information). On the DOPC/DOPE/Chol GUV, where DOPC and DOPE were homogeneously distributed at a micrometer-scale, no binding of DNA was observed in either the absence (Figure 1Ab) or the presence (Figure 1Bb) of Mg^{2+} under the experimental conditions. In contrast, on the DOPC/DPPE/Chol GUV, where DOPC and DPPE were segregated into different domains, the DNAs were bound to the GUV with a characteristic localization pattern in the presence of Mg^{2+} (Figure 1Db). The merged image shows that DNAs were preferentially bound to the DPPE/cholesterol-rich domain (L_o domain) but not to the DOPC-rich domain (L_d domain) (Figure 1Dc) (Under these experimental conditions, phospholipids tended to form aggregates and small vesicles in the presence of Mg^{2+}, and these tended to be adsorbed on the surface of GUVs. On the GUV in Figure 1D, several phospholipid aggregates are adsorbed on the lower part of the GUV, and DNA was bound to some of these phospholipid aggregates. In the upper part of the GUV, phase separation occurred on the unilamellar membrane, and DNA was located only on the DPPE/cholesterol domain; also see images in Figure S1, Supporting Information).

A distinctive characteristic of long DNA (≥20−30 kbp) as a negatively charged semiflexible polymer is that it shows a large discrete conformational transition between a coiled state and highly compact (folded) states, depending on the presence of condensing agents such as polyamine.[21−23] The conformational states (coiled or compact) of individual long DNA molecules in aqueous solution can be observed using a high-speed and ultrasensitive microscope camera under fluorescence microscopy when the DNA is labeled with intercalate-type fluorescent dyes.[24,25] We observed individual T4 DNA molecules in the bulk aqueous solution and on the DOPC/DPPE/Chol GUVs in real time (with a rate of 33 ms/frame) in the presence of spermine (tetravalent amine). A representative fluorescence image (Figure 2a) of T4 DNA molecules and a quasi-three-dimensional representation of fluorescence intensity (Figure 2b) are shown. In the left part of the image of Figure 2a, there is one DNA molecule with a compact conformation, exhibiting Brownian motion in the bulk solution. The density of the fluorescence intensity of this DNA molecule in the image is very high (Figure 2b). In the right part of the image, three DNA molecules with the elongated conformation are located on the surface of a GUV. These three DNA molecules have the profile of lower fluorescence intensity density throughout the entire molecule. We observed more than 20 DNA molecules in the bulk solution and on the GUVs, and the length and mean fluorescence intensity density of each DNA molecule were calibrated (Figure 2d). All of the DNA molecules observed in the bulk solution (25 molecules) had the highly compact conformation, as we previously reported,[24,25] which gives the short molecular length (0.7 ± 0.2 μm) in Figure 2d. As for the fluorescence intensity (1.1 ± 0.53 in arbitrary units) of the molecule, there is a relatively large variation among the molecules. The DNA

DOI: 10.1021/jz101376m | J. Phys. Chem. Lett. 2010, 1, 3391–3395

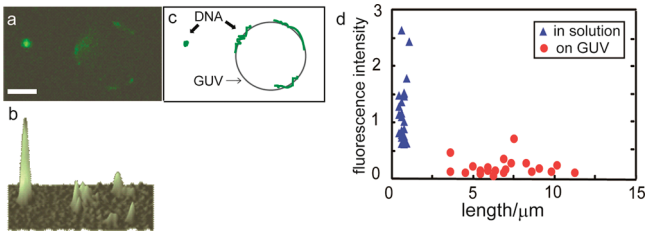

Figure 2. T4 DNA molecules in the bulk solution and on a DOPC/DPPE/Ch GUV with 2 mM $MgCl_2$ and 0.1 mM spermine. (a) Fluorescence image, (b) quasi-three-dimensional representation of fluorescence intensity for image (a), (c) schematic representation of image (a). A time series of fluorescence images of T4 DNA molecules was obtained at a rate of 33 ms/frame with an EM-CCD camera, and one frame is shown. The focus was on the center plane in the *z*-axis of the GUV. Scale bar, 5 μm. (d) Correlation between the fluorescence intensity and the molecular long-axis length of DNAs in bulk solution (triangular) and on GUV (circle). Each spot represents one DNA molecule. The fluorescent intensity corresponds to the height as exemplified in (b) and is given in arbitrary units.

molecules in the bulk aqueous solution exhibited very fast translational Brownian motion and were captured as the clearly visible image only during several to ten frames (the period of less than 0.33 s). Even during the period corresponding to a single video image (33 ms), the molecules appeared not to stay on the just focus position in the image. The large variation of fluorescence intensity shown in Figure 2d reflects such a "de-focusing effect".

The DNA molecules on the GUVs had the longer length (6.9 ± 2.1 μm; the number of molecules, 20) and the lower fluorescence intensity density (0.2 ± 0.15 in arbitrary units), which is clearly distinct from those of the DNAs in the bulk solution (Figure 2d). On the GUVs, some DNA molecules seemed to be completely unfolded while others seemed to be partly unfolded, which would give the relatively large variation in the estimated length (also, it is actually somewhat difficult to estimate the accurate molecular length from the images of DNA on a GUV in aqueous solution, the diameter of which is not significantly longer compared to the length of the elongated DNA molecule). These results clearly indicate that the DNA molecules exhibited a conformational transition accompanied by the attachment to the membrane surface. A similar phenomenon of a specific change in the conformation and location of DNA from a compact state in the aqueous phase to an elongated state on the membrane surface has been observed in a water droplet covered with DOPE monolayer.[25]

The results are schematically summarized in Figure 3. DNA was not bound to the GUV composed of DOPC and DOPE with cholesterol, where they were uniformly distributed with respect to each other and the membrane had a homogeneous phase (A). The DNAs existed in the aqueous solution with a compact conformation. When the membrane structure was segregated to cause a L_o domain enriched with a saturated DPPE, DNAs were preferentially bound to the DPPE-rich L_o domain with an elongated conformation (B).

The binding of DNA to a zwitterionic phospholipid membrane in the presence of Mg^{2+} or Ca^{2+} has been explained in terms of ion adsorption; the lipid head groups become positively charged upon the binding of Mg^{2+} or Ca^{2+} to the

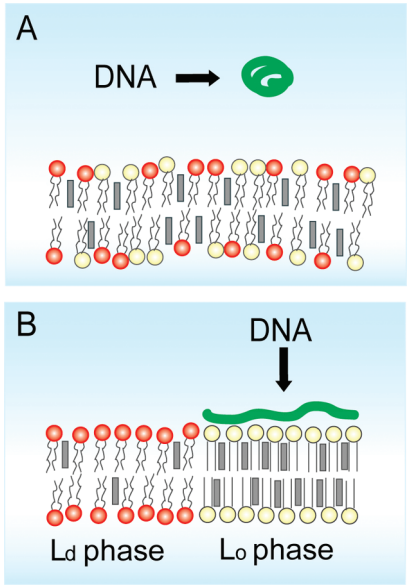

Figure 3. Schematic representation of the results; interaction of DNA with a phospholipid bilayer membrane. (A) red, DOPC; yellow, DOPE; gray (rectangular), cholesterol; green, a DNA molecule with a compact conformation. (B) red, DOPC; yellow, DPPE; gray (rectangular), cholesterol; green, a DNA molecule with an elongated conformation.

phosphate moiety of the phospholipid, and thus, the membrane interacts with negatively charged DNA.[16−20] To make the binding state of DNA on the membrane sufficiently stable, the translational entropy loss of the DNA molecule caused by localization from the three-dimensional aqueous solution to the two-dimensional membrane surface should be compensated for by the gain in free energy due to DNA−phospholipid interaction.

The surface charge density of the membrane is a crucial factor for the DNA−phospholipid membrane interaction. In the L_o phase, it is considered that the surface charge density becomes higher than that in the L_d phase because of the higher packing density of phospholipids. Also, through the experiment on a water-in-oil microdroplet covered by a lipid film, we recently observed that T4 DNA is bound to a DOPE monolayer but not to an egg yolk PC (mainly composed of PC with unsaturated acyl chains) monolayer at a fixed Mg^{2+} concentration,[25] suggesting that DNA interacts stronger with a PE membrane than with a PC membrane in the presence of Mg^{2+} due to the smaller volume of the head group (ethanolamine residue) of PE than that (choline residue) of PC. Our present observation is interpreted as that: The phase separation generated a region with high surface charge density (a L_o domain enriched in DPPE) on the membrane, which was sufficient to attract the DNA molecule onto the membrane surface through the electrostatic interaction. The DNA−membrane interaction would become stronger as the area of contact between DNA and the membrane increases, which makes a DNA molecule with an elongated conformation stable on the membrane surface.

There have been many reports that the binding of macromolecules such as proteins to cationic phospholipids on a

DOI: 10.1021/jz101376m | *J. Phys. Chem. Lett.* **2010**, *1*, 3391–3395

membrane induces a phase separation.[26−30] In contrast, the present results demonstrate that phase separation due to the difference in the acyl chain configuration of phospholipids generates segregated fields with different characteristics regarding the surface charge density. Thus, the phase-separated membrane induces the binding of DNA with an elongated conformation to specific sites on the segregated membrane. Our finding, that is, the coupling of phase separation on a phospholipid membrane with a structural transition of a semiflexible polymer on the membrane surface, is of scientific significance not only from the point of view of the macromolecule−membrane interaction but also to gain deeper insight into the roles of heterodomain structures on cellular membranes.

EXPERIMENTAL SECTION

1,2-Dioleoyl-*sn*-glycero-3-phosphatidylcholine (DOPC), 1,2-dioleoyl-*sn*-glycero-3-phosphatidylethanolamine (DOPE), 1,2-dipalmitoyl-*sn*-glycero-3-phosphatidylethanolamine (DPPE), and cholesterol were obtained from Wako Pure Chemical Industries (Osaka, Japan), and 1,2 dioleoyl-*sn*-glycero-3-phosphoethanolamine-*N*-(lissamine rhodamine B sulfonyl) (rhodamine-DOPE) was from Avanti Polar Lipids (Alabaster, AL). Giant unilamellar vesicles (GUV) were prepared by the natural swelling method.[12] A lipid film composed of 30 μmol of DOPC, 30 μmol of DOPE or DPPE, 35 μmol of cholesterol, and 0.06 μmol of rhodamine-DOPE was made at the bottom of a glass tube; 1 mL of Milli-Q-water was added, and the mixture was allowed to stand for 4 h at 37 °C for DOPC/DOPE/cholesterol/rhodamine-DOPE GUVs or at 67 °C for DOPC/DOPE/cholesterol/rhodamine-DOPE GUVs. The resultant GUV solution was stored at room temperature. T4 DNA was obtained from Nippon Gene (Tokyo, Japan) and labeled with YOYO-1 iodide (Invitrogen, Carlsbad, CA), as described previously.[25] The molar ratio of nucleotides to YOYO-1 was ∼10:1.

Confocal laser scanning fluorescence microscope images were obtained by Carl Zeiss LSM510 coupled with an argon laser (LGK7812ML4, Lasertechnik, Jena, Germany) and a 543 nm helium−neon laser (LGK 7786, Lasertechnik). An equal volume of 10 ng/μL of T4 DNA labeled with YOYO-1 was added to the GUV solution. The 488 and 543 nm laser lines were simultanoeusly used to irradiate the T4 DNA-GUV solution on a coverslip, and a YOYO-1 image and a rhodamine-DOPE image were simultanoeusly obtained at each fluorescence channel through a 505−530 nm band-pass filter and 585 nm long-pass filter, respectively. The image acquisition time was 1.57 s.

The single-molecule observation of T4 DNA was performed, as described previously.[25] An equal volume of 1 ng/μL of T4 DNA labeled with YOYO-1 in Milli-Q-water containing 4 mM $MgCl_2$ and 0.2 mM spermine (Nacalai Tesque, Kyoto, Japan) was added to the GUV solution. The fluorescence images of individual T4 DNA molecules were obtained with an EM-CCD camera (DU897E, Andor Technology Japan, Tokyo, Japan) and CSUX-1 confocal scanner unit (Yokogawa Manufacturing, Musashino, Japan) coupled with the 488 nm line of a solid-state laser (85-BCD-030-053, Melles Griot, Carlsbad, CA). Image aquision was performed at 33 ms/frame (30 frames/s). The molecular long-axis length and the mean density of the fluorescence intensity of each DNA molecule shown in Figure 2 were estimated on the fluorescence image of a single video frame.

SUPPORTING INFORMATION AVAILABLE Additional fluorescence microscope images of GUVs with DNAs. This material is available free of charge via the Internet at http://pubs.acs.org.

AUTHOR INFORMATION

Corresponding Author:

*To whom correspondence should be addressed. Phone: +81-75-753-3671. Fax: +81-75-753-3779. E-mail: yoshikaw@scphys.kyoto-u.ac.jp.

ACKNOWLEDGMENT This work was partly supported by the Japan Society for the Promotion of Science (JSPS) under a Grant-in-Aid for Creative Scientific Research (Project No. 18GS0421) and by the Sasagawa Scientific Research Grant from the Japan Science Society to A.K. M.Y. is grateful for support from the Japan Society for the Promotion of Science (Grant-in-Aid for JSPS Fellows; No. 22-940). The authors thank Dr. Yuko Sato, Kyoto University, for her helpful discussion.

REFERENCES

(1) Edidin, M. Lipid Microdomains in Cell Surface Membranes. *Curr. Opin. Struct. Biol.* **1997,** *7*, 528–532.
(2) Lagerholm, B. A.; Weinreb, G. E.; Jacobson, K.; Tompson, N. Detecting Microdomains in Intact Cell Membranes. *Annu. Rev. Phys. Chem.* **2005,** *56*, 309–336.
(3) Cheng, Z. J.; Singh, R. D.; Marks, D. L.; Pagano, R. E. Membrane Microdomains, Caveolae, and Caveolar Endocytosis of Sphingolipids. *Mol. Membr. Biol.* **2006,** *23*, 101–110.
(4) Day, C. A.; Kenworthy, A. K. Tracking Microdomain Dynamics in Cell Membranes. *Biochim. Biophys. Acta* **2009,** *1788*, 245–253.
(5) Simons, K.; Gerl, M. J. Revitalizing Membrane Rafts: New Tools and Insights. *Nat. Rev. Mol. Cell Biol.* **2010,** *11*, 688–699.
(6) Garcia-Marcos, M.; Dehaye, J.-P.; Marino, A. Membrane Compartments and Purinergic Signalling: the Role of Plasma Membrane Microdomains in the Modulation of P2XR-Mediated Signalling. *FEBS. J.* **2009,** *276*, 330–340.
(7) He, H.-T.; Marguet, D. T-Cell Antigen Receptor Triggering and Lipid Rafts: A Matter of Space and Time Scales. *EMBO Rep.* **2008,** *9*, 525–530.
(8) Korlach, J.; Schwille, P.; Webb, W. W.; Feigenson, G. W. Characterization of Lipid Bilayer Phases by Confocal Microscopy and Fluorescence Correlation Spectroscopy. *Proc. Natl. Acad. Sci. U.S.A.* **1999,** *96*, 8461–8466.
(9) Scherfeld, D.; Kahya, N.; Schwille, P. Lipid Dynamics and Domain Formation in Model Membranes Composed of Ternary Mixture of Unsaturated and Saturated Phosphatidylcholines and Cholesterol. *Biophys. J.* **2003,** *85*, 3758–3768.
(10) Veatch, S. L.; Keller, S. L. Separation of Lipid Phases in Giant Vesicles of Ternary Mixtures of Phospholipids and Cholesterol. *Biophys. J.* **2003,** *85*, 3074–3083.
(11) Veatch, S. L.; Keller, S. L. Seeing Spots: Complex Phase Behaviour in Simple Membranes. *Biochim. Biophys. Acta* **2005,** *1746*, 172–185.
(12) Hup, H. H.; Zimmermann, U.; Ringsdort, H. Preparation of Large Unilamellar Vesicles. *FEBS Lett.* **1982,** *140*, 254–256.
(13) Baumgart, T.; Hunt, G.; Farkas, E. R.; Webb, W. W.; Feigenson, G. W. Fluorescence Probe Partitioning Between L_o/L_d Phases

DOI: 10.1021/jz101376m | *J. Phys. Chem. Lett.* **2010,** *1*, 3391–3395

in Lipid Membranes. *Biochim. Biophys. Acta* **2007,** *1768*, 2182–2194.
(14) Saeki, D.; Hamada, T.; Yoshikawa, K. Domain-Growth Kinetics in a Cell-Sized Liposome. *J. Phys. Soc. Jpn.* **2006,** *75*, 013602.
(15) Cans, A.-S.; Andes-Koback, M.; Keating, C. D. Positioning Lipid Membrane Domains in Giant Vesicles by Micro-organization of Aqueous Cytoplasm Mimic. *J. Am. Chem. Soc.* **2008,** *130*, 7400–7406.
(16) Lis, L. J.; Lis, W. T.; Parsegian, V. A.; Rand, R. P. Adsorption of Divalent Cations to a Variety of Phosphatidylcholine Bilayers. *Biochemistry* **1981,** *20*, 1771–1777.
(17) Herbette, L.; Napolitano, C.; McDaniel, R. Direct Determination of the Calcium Profile Structure for Dipalmitoyllecithin Multilayers Using Neutron Diffraction. *Biophys. J.* **1984,** *46*, 677–685.
(18) Gromelski, S.; Brezesinski, G. DNA Condensation and Interaction with Zwitterionic Phospholipids Mediated by Divalent Cations. *Langmuir* **2006,** *22*, 6293–6301.
(19) Tresset, G.; Cheong, W. C. D.; Lam, Y. M. Role of Multivalent Cations in the Self-Assembly of Phospholipid−DNA Complexes. *J. Phys. Chem. B* **2007,** *111*, 14233–14238.
(20) Mengistu, D. H.; Bohinc, K.; May, S. Binding of DNA to Zwitterionic Lipid Layers Mediated by Divalent Cations. *J. Phys. Chem. B* **2009,** *113*, 12277–12282.
(21) Bloomfield, V. A. Electrostatic Effects on the Stability of Condensed DNA in the Presence of Divalent Cations. *Curr. Opin. Struct. Biol.* **1996,** *6*, 334–341.
(22) Mel'nikov, S. M.; Sergeyev, V. G.; Yoshikawa, K. Discrete Coil−Globule Transition of Large DNA Induced by Cationic Surfactant. *J. Am. Chem. Soc.* **1995,** *117*, 2401–2408.
(23) Takahashi, M.; Yoshikawa, K.; Vailevskaya, V. V.; Khokhlov, A. R. Discrete Coil−Globule Transition of Single Duplex DNAs Induced by Polyamine. *J. Phys. Chem. B* **1997,** *101*, 9396–9401.
(24) Makita, N; Ullner, M.; Yoshikawa, K. Conformational Change of Giant DNA with Added Salt as Revealed by Single Molecular Observation. *Macromolecules* **2006,** *39*, 6200–6206.
(25) Kato, K.; Shindo, E.; Sakaue, T.; Tsuji, A.; Yoshikawa, K. Conformational Transition of Giant DNA in a Confined Space Surrounded by a Phspholipid Membrane. *Biophys. J.* **2009,** *97*, 1678–1686.
(26) Mitraskos, P.; Macdonald, P. M. Domains in Cationic Lipid Plus Polyelectrolyte Bilayer Membranes: Detection and Characterization via 2H Nuclear Magnetic Resonance. *Biochemistry* **1996,** *35*, 16714–16722.
(27) Radler, J. O.; Koltover, L.; Salditt, T.; Safinya, C. R. Structure of DNA−Cationic Liposome Complexes: DNA Intercalation in Multilamellar Membranes in Distinct Interhelical Packing Regimes. *Science* **1997,** *275*, 810–814.
(28) Heimburg, T.; Angerstein, B.; Marsh, D. Binding of Peripheral Proteins to Mixed Lipid Membranes: Effect of Lipid Demixing upon Binding. *Biophys. J.* **1999,** *76*, 2575–2586.
(29) Hammond, A. T.; Heberle, F. A.; Baumgart, T.; Barid, B.; Feigenson, G. W. Crosslinking a Lipid Raft Component Triggers Liquid Ordered−Liquid Disordered Phase Separation in Model Plasma Membranes. *Proc. Natl. Acad. Sci. U.S.A.* **2005,** *102*, 6320–6325.
(30) Liu, A. P.; Fletchler, D. A. Actin Polymerization Serves as a Membrane Domain Switch in Model Lipid Bilayers. *Biophys. J.* **2006,** *91*, 4064–4070.

DOI: 10.1021/jz101376m | *J. Phys. Chem. Lett.* **2010,** *1*, 3391–3395